Optical Characterisation of $La_{0.7}Sr_{0.3}MnO_3$ Thin Film Based Uncooled Bolometers

Ammar Aryan[1,2,3,*], Jean-Marc Routoure[1,2,3,+], Bruno Guillet[1,2,3,+], Pierre Langlois[1,2,3,+], Cédric Fur[1,2,3,+],
Julien Gasnier[1,2,3,+], Carolina Adamo[4,#], Darrell G. Schlom[4,5,##] and Laurence Méchin[1,2,3,+]

[1] Université de Caen Basse-Normandie, UMR 6072 GREYC, F-14032 Caen, France
[2] ENSICAEN, UMR 6072 GREYC, F-14050 Caen, France
[3] CNRS, UMR 6072 GREYC, F-14032 Caen, France
[4] Department of Materials Science and Engineering, Cornell University, Ithaca, New York 14853-1501, USA
[5] Kavli Institute at Cornell for Nanoscale Science, Ithaca, New York 14853, USA
[+] Email addresses: first-name.name@unicaen.fr
[#] Email address: ca259@cornell.edu
[##] Email address: schlom@cornell.edu
[*] Corresponding author: ammar.aryan@unicaen.fr

Abstract— **This paper reports the potentialities of the manganese oxide $La_{0.7}Sr_{0.3}MnO_3$ (LSMO) for the realization of uncooled thermal detectors. Close to room temperature, LSMO exhibits a metal-to-insulator transition, where a large change of electrical resistance versus temperature occurs. The tested sample is a 100 nm thick epitaxial LSMO thin film deposited on a $SrTiO_3$ buffered Si substrate. The optical responsivity and electrical noise were measured in a frequency range of 1 Hz-100 kHz, thus enabling the estimation of specific detectivity. It is shown that due to the very low 1/f noise level, in this epitaxial film deposited on silicon wafer, LSMO thermal detectors can exhibit competitive performances at room temperature.**

Keywords- Bolometer; manganite; thermal detector.

I. INTRODUCTION

Uncooled infrared (IR) detectors have been studied in recent years due to a variety of applications such as thermal cameras, night vision cameras, thermal sensors, surveillance, etc. The IR detectors are generally sorted in two types: photon detectors and thermal detectors. The photon detectors have high signal to noise ratio and very fast response, but require generally a cooling system, which is heavy and expensive. In comparison with photon detectors, most of thermal detectors operate at room temperature, thus reducing the cost of operation. Even its response time is still larger than that of photon detectors, it has no limitation on the wavelength response band. Thus makes it possible to be used for hand-held infrared applications.

Thermal detectors are based on three different approaches, namely, bolometers, pyroelectric and thermoelectric effects. Uncooled microbolometers take a large part of infrared imaging application business [1]. A bolometer is a thermal detector whose electrical resistance R changes as a function of radiant energy. So, the larger the resistance changes, the higher the Temperature Coefficient of Resistance ($\beta = 1/R \times dR/dT$ expressed in K^{-1}), and the higher the responsivity. Many materials such as metals (Au, Pt, Ti, *etc.*) [2][3], and semiconductors (VO_x, amorphous silicon, *etc.*) [4][5] have been used as thermometer in uncooled bolometers.

The rare earth manganese oxides may find important applications such as magnetic random access memories and magnetic sensors [6][7]. It has been realized that these materials have a promising potential for bolometric infrared detection [8][9]. The large change of their electrical resistance R at the metal-to-insulator transition, which takes place in the 300-350 K range, makes them potential materials for the fabrication of uncooled thermal detectors. Ideal materials would present, at the desired operating temperature T close to 300 K, a high β and a low noise level.

Even if it does not exhibit the highest β values at room temperature, compared to other possible manganite compositions, we study $La_{0.7}Sr_{0.3}MnO_3$ (LSMO) because it shows low 1/f noise and no excess noise at the metal-to-insulator transition [9]-[15]. In addition, we use a good quality LSMO films deposited on silicon substrates, which enables the compatibility with silicon microelectronic fabrication process and possible development of more complex systems.

In section II we will describe the sample fabrication details together with the measurement setup. The third section is dedicated to the theoretical principle of operation of bolometer, and to the definitions of figures of merits. Then, in the fourth section, we will show detailed electrical and optical characterizations of the tested sample, with comparison to other uncooled bolometers. Finally, a conclusion section is devoted to show the potentialities of LSMO/STO/Si thin films as promising uncooled thermal detector.

II. EXPERIMENTAL DETAILS

A. Sample preparation

The sample consists in a 100 nm thick epitaxial LSMO thin film deposited on SrTiO$_3$ (20 nm thick) buffered Si (001) substrates by reactive molecular beam epitaxy [16]. After gold deposition, the film was patterned using standard UV photolithography and argon ion milling. Ultrasonic bonding was used to connect the gold contacts to the sample holder.

Our sample, shown in Fig. 1, has a meander line shape with the overall pixel dimension of 150×230 µm². The meander line width is 50 µm. The meander filling factor (defined as the ratio of the area occupied by the LSMO meander to the device nominal area) is equal to 91%.

B. Measurement setup

A semiconductor laser diode (635 nm, 5 mW) electronically modulated at different frequencies was used to optically heat the device. The laser beam was collimated and passed through a 1:1 beam splitter with one beam incident on a photodiode and the other incident on the studied sample. Thus, by knowing the transmission coefficient of all optical elements, the power of the incident light on the sample can be directly obtained by measuring the photodiode output signal. The laser diode spot has an elliptical shape, with dimensions of 128 µm × 186 µm estimated at Full Width Half Maximum.

The sample was glued to a copper plate, having a heating element, then fixed into a vacuum chamber equipped with an optical window. The chamber is evacuated by a mechanical pump, and no cooling system was used. A temperature controller was used to maintain temperature stability of 15 mK during measurements at fixed temperature. The controller, also, provides the possibility of heating the sample in the range 300-350 K.

The LSMO sample was current biased using a quasi-ideal DC current source, which exhibits very high output impedance and a negligible noise contribution [17]. A standard four-probe technique was used to provide bias current and measure the voltage signal of the LSMO sample. The output voltage of the sample was read out by a homemade voltage amplifier. The dynamic optical response and electrical noise measurements were carried out using a spectrum analyser (HP3562A). The measurement setup is equipped with personal computer with GPIB interface to read and store the measured values.

III. BOLOMETER BACKGROUND

A. Principle of operation

When the bolometer material absorbs an amount Q of radiated power from a light source, a temperature change ΔT occurs: $\Delta T = \eta Q / G_{eff}$, where G_{eff} is the effective thermal conductance of bolometer material (expressed in
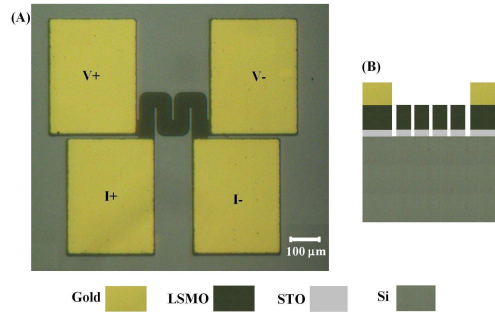

Figure 1. (A) Optical photography of the tested sample with the two current probes [I+, I-] and two voltage probes [V+, V-]. (B) Schematic cross-section of the sample.

W·K^{-1}), and η is the absorption coefficient (dimensionless). G_{eff} is related to the self-heating effect and given by the relation: $G_{eff} = G - I_b^2 \times (dR/dT)$, where G is the geometrical thermal conductance of the bolometer. The variation of the temperature causes a change in the electrical resistance R of the bolometer material:

$$\Delta R = \beta R \times \Delta T = \beta R \times \eta Q / G_{eff} \qquad (1)$$

So, when using a bias current I_b through such a bolometer, a voltage change can be measured:

$$\Delta V = (I_b \beta R \eta Q) / G_{eff} \qquad (2)$$

B. Figures of merit

The performance of bolometers is expressed in terms of device figures of merit such as optical responsivity ($\Re_v$), Noise Equivalent Power (NEP), specific detectivity (D*), and β [18].

The optical responsivity ($\Re_v$) of a bolometer is defined as the output voltage per radiated power when bias current I_b is applied to the bolometer device, and is written as:

$$\Re_v(\omega) = \frac{\Delta V}{\Delta Q} = \frac{\eta I_b}{G_{eff}(1+\omega^2 \tau_{eff}^2)^{1/2}} \frac{dR}{dT} \quad [V.W^{-1}] \quad (3)$$

where $\tau_{eff} = C / G_{eff}$ is the effective thermal time constant, and C is the thermal capacitance of the bolometer.

The NEP (expressed in W·Hz$^{-1/2}$) is defined as the incident power on a pixel that generates a signal-to-noise ratio equal to unity in a 1 Hz output bandwidth. The NEP of the bolometer is calculated as the ratio of the square root of the voltage noise spectral density ($S_v^{1/2}$) over the bolometer responsivity ($\Re_v$).

The D* (expressed in cm·Hz$^{1/2}$·W^{-1}) provides information that is equivalent to NEP, but with the possibility to compare bolometer pixels of different areas. It is calculated as the ratio of the square root of effective surface of bolometer (expressed in cm²) over the NEP.

Another important figure of merit is the impulse detectivity [19], which is defined as $D^*/\tau_{eff}^{1/2}$ (expressed in $cm \cdot J^{-1}$). This parameter illustrates the necessary compromise between optical responsivity and effective time thermal constant.

IV. RESULTS AND DISCUSSION

A. Electrical characteristics

The electrical resistance versus temperature (R-T) data of the LSMO sample was measured using a standard four-point technique. Then the R-T data were fitted with a smooth equation and then the dR/dT and β data were calculated and plotted as seen in Fig. 2 and Fig. 3. The maximum β value obtained is 2.7×10^{-2} K^{-1}, which is a typical value for the LSMO material [10][11]. We can estimate the electrical resistivity of about 2.4×10^{-5} $\Omega \cdot m$ at 300 K, which is close to literature value for this material [20].

The R-T plot presents a non linear shape. So, in order to get maximum responsivity, the sample should be characterised at a temperature where we have the maximum of dR/dT (Fig. 3). The maximum dR/dT value equals 85 $\Omega \cdot K^{-1}$ at 318 K, so the sample will be optically characterised at this temperature (and not at the temperature where β is maximal).

B. Optical responsivity

In order to identify whether the optical responsivity is bolometric (thermal), we have compared it with dR/dT as a function of the temperature (Fig. 3). It is found that the dependence of optical responsivity $(\Re_v)$ at 1 Hz on the temperature follows well the variation of dR/dT versus temperature, and they reach a maximum value at the same temperature 318K. This suggests that the major component of the response at 1 Hz is bolometric.

C. Dynamic characterisations

Figure 4 shows the dependence of the optical responsivity as a function of the laser power modulation frequency for different bias currents. We have an optical responsivity of 0.65 $V \cdot W^{-1}$ at 1 Hz for the bias current equals to 400 µA.
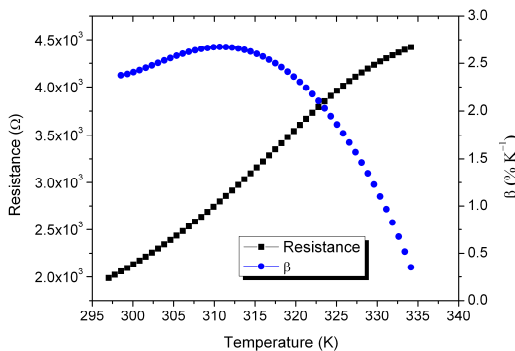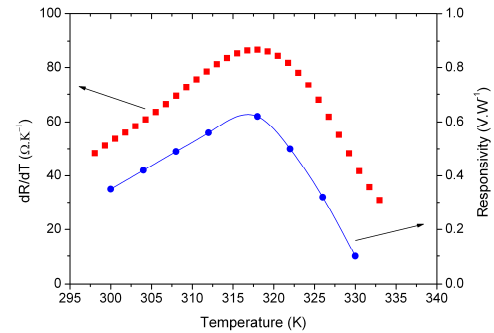
Figure 3.   Optical responsivity $\Re_v$ at bias current 400 µA and frequency 1 Hz and dR/dT versus temperature curves.

Three different behaviours can be observed in Fig. 4. From 1 Hz up to the cut-off frequency (around 1 kHz), the optical responsivity is almost constant, whatever is the value of I_b. In the 1-10 kHz decade, we observe a low-pass behaviour and then an increasing of the optical responsivity as function of frequency. Equation (3) can be used to identify the plateau and the low pass filtering. Inset of Fig. 4 shows that the optical responsivity increases linearly with increasing the bias current, according to (3).

We do not observe a constant plateau in our experiment. One possible explanation could be the heat diffusion across the substrate. The increasing optical responsivity at higher frequencies (more than 1 kHz) could be related to the contribution of photo-induced effects in LSMO or in the LSMO/STO/Si heterostructure [8][21]. Further studies are in progress to characterize this non-bolometric component.

An optical step of incident power light was applied at the sample, and then the output voltage time-response of sample was measured. Thus, we can extract the effective thermal time constant τ_{eff} of the sample by using the fitting of sample's time-response as a first order system. We found that τ_{eff} is of the order of 180 µs, which is consistent with the measured cut-off frequency (Fig. 4). This effective thermal time constant is quite short for a thin film bolometers [8][21][22].

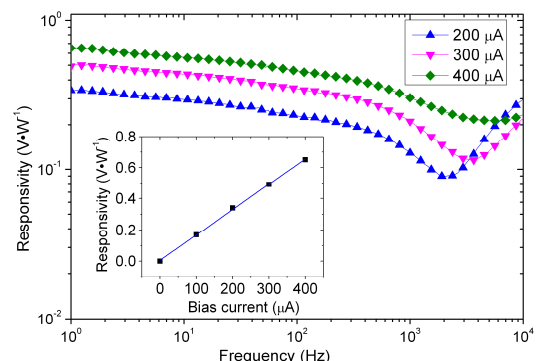Figure 2.   Sample's electrical resistance and β versus temperature

Figure 4.   Optical responsivity versus laser modulation frequency at different bias currents at 318 K. The inset shows optical responsivity versus bias current at 1 Hz and 318 K
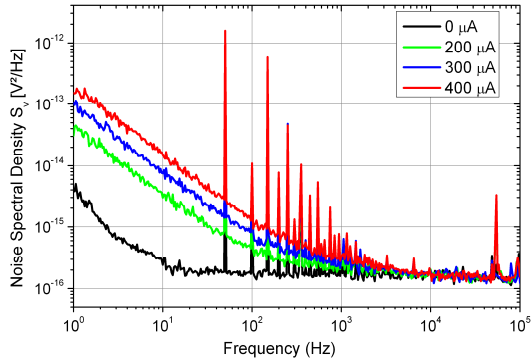
Figure 5.   Noise spectral density measured in the four probe configuration at different bias currents at 318K.

We can also estimate $G = 47\times10^{-3}$ W·K^{-1} by using (3) in the pass-band frequencies, and using the value of absorption η=85% from earlier measurements on this material [9][20]. We found that $G_{eff} = G$ at bias current equals 400 µA. By knowing the thermal time constant and the thermal conductance, we can estimate the thermal capacitance of our sample $C=8.5\times10^{-6}$ J·K^{-1}.

D. Noise, NEP and D*

The voltage noise spectral density (S_v) of the sample was measured using the four-probe configuration for different values of the bias current at 318 K, as shown in Fig. 5.

As expected, the white noise level does not depend on the bias current and the 1/f noise increases with bias current. Measurement results give a value of S_v equals to 4.4×10^{-15} V^2·Hz^{-1} at 30 Hz, for bias current equals to 400 µA. Using the value of the optical responsivity, we can estimate the value of NEP and D*. The measured NEP and D* value at 318 K, 400 µA and 30 Hz, are 1.1×10^{-7} W·Hz$^{-1/2}$ and 1.7×10^{5} cm·Hz$^{1/2}$·W^{-1} respectively.

Table I presents a comparison with other manganite material bolometer [23]. We notice that our sample present better optical responsivity at the same bias current (1.95 V·W^{-1} at 1.2 mA, using (3)) even it has a smaller surface. So, in terms of optical responsivity, LSMO bolometer presents a better performance than LPSMO. Also, even if our sample has smaller D*, it presents a smaller effective time constant (τ_{eff}). So, in terms of impulse detectivity, which includes both parameters, our sample achieves same value as that of [23], but with a decrease of about 4 factor in Joule heating.

The summary of results of the tested bolometer, with comparison of other uncooled bolometers, is shown in Table II. We can note that the D* of our sample is still limited compared to these bolometer materials, like Poly-SiGe [24] and VOx [25], but our sample present better time response. It is also still limited in terms of impulse detectivity. This is mainly related to the fact that other bolometers used suspended structures, which decrease the thermal conductance (about 10^{-7} W·K^{-1}), thus

enhancing the specific detectivity by about 4 orders of magnitude.

V.   CONCLUSION

In this paper, the potentialities of LSMO thin films as thermal detector at room temperature have been reported. We have fabricated and characterized the LSMO/STO/Si sample at an operating temperature of 318 K. The sample showed high β (24×10^{-3} K^{-1}) and low electrical noise.

The sample presents a very good quality LSMO film deposited on Si substrate. This proves the compatibility with silicon microelectronic fabrication process, and gives the opportunity to the integration of LSMO as uncooled thermal detector with the readout electronics.

Figures of merits of bolometer have been measured and analyzed. It showed that due to a thermal conductance of 47×10^{-3} W·K^{-1}, the device performance is limited to a D* of 1.7×10^{5} cm·Hz$^{1/2}$·W^{-1} at 30 Hz and 400 µA. Though, a small effective thermal time constant of 180µs was measured.

Further studies are in progress to optimize the geometrical parameters of the sample, like size and number of lines in the meander, and on different substrates in order to achieve maximal performance of this promising material as thermal detector.

TABLE I.   COMPARISON WITH OTHER MANGANITE BOLOMETERS

	This work	**Ref. [23]**
Film/Substrate	LSMO/STO/Si	LPSMO*/LaAlO$_3$
Pixel pitch size (µm×µm)	150×230	2500×3000
β (%K^{-1})	2.4 @318K	5.5 @300K
G (W·K^{-1})	47×10^{-3}	3×10^{-3}
I$_b$ (mA)	0.4	1.2
R·I$_b^2$ (mW)	0.34	1.58
$\Re v$ (V·W^{-1})	0.65	0.60
τ_{eff}	180 µs	500 ms
NEP at 30Hz (W·Hz$^{-1/2}$)	1.1×10^{-7}	3.0×10^{-8}
D* at 30Hz (cm·Hz$^{1/2}$·W^{-1})	1.7×10^{5}	9.0×10^{6}
D*/$\tau_{eff}^{1/2}$ (cm·J^{-1})	1.3×10^{7}	1.3×10^{7}

*LPSMO : La$_{0.7}$(Pb$_{0.63}$Sr$_{0.37}$)$_{0.3}$MnO$_3$

TABLE II. COMPARISON WITH OTHER UNCOOLED BOLOMETERS

	This work	**Ref. [24]**	**Ref. [25]**
Film/Substrate	LSMO/STO/Si	Poly-SiGe/Si	VO_x/Si
Structure	not suspended meander	suspended microbridge	suspended microbridge
Pixel pitch size ($\mu m \times \mu m$)	150×230	50×60	50×60
Resistance at 300K (kΩ)	2.13	350	50
β at 300K (%K^{-1})	1.9	-1.9	-2.1
G (W.K^{-1})	47×10^{-3}	1×10^{-6}	1×10^{-5}
R·I$_b^2$ (mW)	0.34	0.45	0.50
τ_{eff}	180 μs	16.6 ms	3 ms
D* at 30Hz (cm·Hz$^{1/2}$·W^{-1})	1.7×10^5	7.5×10^8	2×10^8
D*/$\tau_{eff}^{1/2}$ (cm·J^{-1})	1.3×10^7	5.8×10^9	3.7×10^9

REFERENCES

[1] J.L. Tissot, "IR detection with uncooled sensors", Infrared Phys. Techn., 46, pp. 147-153, 2004.

[2] K.C. Liddard, "Thin-film resistance bolometer IR detectors", Infrared Phys., pp. 57–64, 1984.

[3] A. Tanaka, S. Mastsumoto, N. Tsukamoto, S. Itoh, and K. Chiba, "Infrared focal plane array incorporating silicon IC process compatible bolometer", IEEE Trans. Electron. Dev., vol. 43, pp. 1844–1850, 1996.

[4] H. Jerominek, F. Picard, N. Swart, M. Renaud, and M. Levesque, "Micromachined uncooled VO_2-based IR bolometer arrays", Proceedings of SPIE, vol. 2746, p. 60, 1996.

[5] E. Mottin, A. Bain, J.L. Martin, J.L. Ouvrier-Buffet, S. Bisotto, J.J. Yon, and J.L. Tissot, "Uncooled amorphous silicon technology enhancement for 25-µm pixel pitch achievement", Proceedings of SPIE, vol. 4820, pp. 200–207, 2003.

[6] T. Venkatesan, M. Rajeswari, Z.-W. Dong, S. B. Ogale, and R. Ramesh, "Manganite-based devices: opportunities, bottlenecks and challenges", Phil. Trans. R. Soc. Lond. A, vol. 356, no. 1742, pp. 1661–1680, 1998.

[7] S. Wu, D. Fadil, S. Liu, A. Aryan, B. Renault, J. –M. Routoure, S. Flament, P. Langlois, L. Méchin, and B. Guillet, "$La_{0.7}Sr_{0.3}MnO_3$ Thin films for magnetic and Temperature Sensors at Room Temperature ", Sensors & Transducers Journal, vol. 14-1, pp. 253-265, 2012.

[8] M. Rajeswari, C. H. Chen, A. Goyal, C. Kwon, M. C. Robson, R. Ramesh, T. Venkatesan, and S. Lakeou, "Low-frequency optical response in epitaxial thin films of $La_{0.67}Ca_{0.33}MnO_3$ exhibiting colossal magnetoresistance", Appl. Phys. Lett., vol. 68, p. 3555 1996.

[9] L. Méchin, J.-M. Routoure, B. Guillet, F. Yang, S. Flament, D. Robbes, and R. Chakalov, "Uncooled bolometer response of a low noise $La_{2/3}Sr_{1/3}MnO_3$ thin film," Appl. Phys. Lett., vol. 87, p. 204103, 2005.

[10] B. Raquet, J. Coey, S. Wirth, and S. von Moln´ar, "1/f noise in the half-metallic oxides CrO_2, Fe_3O_4, and $La_{2/3}Sr_{1/3}MnO3$," Phys. Rev. B, vol. 59, no. 19, pp. 12435–12443, 1999.

[11] A. Lisauskas, S. Khartsev, and A. Grishin, "Studies of 1/f Noise in $La_{1-x}M_xMnO_3$ (M= Sr, Pb) Epitaxial Thin Films," J. Low Temp. Phys., vol. 117, no. 5, pp. 1647–1651, 1999.

[12] A. Palanisami, R. Merithew, M. Weissman, M. Warusawithana, F. Hess, and J. Eckstein, "Small conductance fluctuations in a second-order colossal magnetoresistive transition," Phys. Rev. B, vol. 66, no. 9, p. 92407, 2002.

[13] L. Méchin, J.-M. Routoure, S. Mercone, F. Yang, S. Flament, and R. Chakalov, 1/f noise in patterned $La_{0.7}Sr_{0.3}MnO_3$ thin films in the 300–400 K range, J. Appl. Phys., vol. 103, p. 083709, 2008.

[14] K. Han, Q. Huang, P. Ong, and C. Ong, "Low-frequency noise in $La_{0.7}Sr_{0.3}Mn_{1-x}Fe_xO_3$ thin films," J. Phys. Condens. Matt., vol. 14, p. 6619, 2002.

[15] F. Yang, L. Méchin, J.-M. Routoure, B. Guillet, and R. A. Chakalov, "Low-noise $La_{0.7}Sr_{0.3}MnO_3$ thermometers for uncooled bolometric applications," J. Appl. Phys, vol. 99, no. 2, p. 024903, 2006.

[16] L. Méchin, C. Adamo, S. Wu, B. Guillet, S. Lebargy, C. Fur, J.-M. Routoure, S. Mercone, M. Belmeguenai, and D. G. Schlom, "Epitaxial $La_{0.7}Sr_{0.3}MnO_3$ thin films grown on $SrTiO_3$ buffered silicon substrates by reactive molecular-beam epitaxy", in press in Phys. Status Solidi A, DOI/10.1002/ ppsa. 201127712, 2012.

[17] J.-M. Routoure, D. Fadil, S. Flament, and L. Méchin, A low-noise high output impedance DC current source, in Proceedings of the 19th International Conference on Noise and Fluctuations; ICNF 2007, AIP Conference Proceedings, vol. 922, no. 1, pp. 419–424, 2007.

[18] P. L. Richards, "Bolometers for infrared and millimeter waves", J. Appl. Phys., vol. 76, p. 1, 1994.

[19] I. A. Khrebtov, "Superconductor Infrared and Submillimeter Radiation Receivers", Sov. J. Opt. Technol., vol. 58, p. 261, 1991.

[20] Y. Okimoto, T. Katsufuji, T. Ishikawa, T. Arima, and Y. Tokura "Variation of electronic structure in $La_{1-x}Sr_xMnO_3$ ($0 \leq x \leq 0.3$) as investigated by optical conductivity spectra", Phys. Rev. B, vol. 55, p. 4206, 1997.

[21] J. H. Hao, X. T. Zeng, and H. K. Wong, "Optical response of single-crystal $(La,Ca)MnO_3$ thin films", J. Appl. Phys. vol. 79, p. 1810, 1996.

[22] J. H. Hao, X. Mao, C. H. Chen, and D. X. Lu, "Room Temperature Bolometric Applications Using Manganese Oxide Thin Films", Int. J. Infrared Millim. Waves, vol. 20, pp. 2113-2120, 1999.

[23] A. Lisauskas, S. I. Khartsev, and Alex Grishin, "Tailoring the colossal magnetoresistivity: $La_{0.7}(Pb_{0.63}Sr_{0.37})_{0.3}MnO_3$ thin-film uncooled bolometer ", Appl. Phys. Lett., vol. 77, p. 756 (2000)

[24] L. Dong, R. Yue, and L. Liu, "An uncooled microbolometer infrared detector based on poly-SiGe thermistor", Sens. Actuators A, vol. 105, pp. 286-292, 2003.

[25] H. Wang, X. Yi, G. Huang, J. Xiao, X. Li, and S. Chen, "IR microbolometer with self-supporting structure operating at room temperature", Infrared Phys. Techn., vol. 45, pp. 53-57, 2003.